Acta Technica *62* (2017), No. 7A, 421–428 © 2017 Institute of Thermomechanics CAS, v.v.i.

An evaluation method of distribution width enhancement mechanism based on density functional theory solution set

Zhenhua Xie[1], Shyam Kattel[2], Li Zhang[1,*]

Abstract. Dry reforming of methane (DRM) provides opportunities of using CH_4 and CO_2 to produce syngas for the Fischer-Tropsh (F-T) synthesis. Density functional theory calculation (DFT) provides *ab initio* insights into the mechanistic and energistic evaluation of DRM in terms of molecular or atom. The results predict that Pt-ter-PtCo(111) surface is more active for the DRM reaction than the Pt(111), mixed-PtCo(111) and Co(001) surfaces. In addition, the calculated free energy diagrams indicate that methane reforming over the bimetallic and monometallic model surfaces are most likely dominated by the first C-H bond activation of methane.

Key words. Dry reforming of methane (DRM), Density functional theory (DFT), Pt-Co..

1. Introduction

Dry reforming of methane (DRM) has attracted increasing attention due to its concurrent conversion of CH_4 and CO_2 (green-house gas) into syngas ($CO + H_2$) for Fischer-Tropsh (F-T) synthesis [1–3]. It has been well documented that noble metals and Ni based catalysts showed good activity to DRM, while they are limited to availability and coke resistance, respectively [3, 4]. Recently, Co-based catalysts also drawn much attention due to its promising catalytic performance [5].

Based on the density functional theory (DFT) calculations, Jones et al. [6] revealed that cobalt shows a relatively high binding strength to oxygen. In addition, it has been reported that oxidation would be one of the reasons (coke deposition, metal sintering, et al.) for the deactivation of the Co-based catalysts [7]. Thus, measures to

[1]College of Power Engineering, Chongqing University, Chongqing 400044, China
[2]Chemistry Department, Brookhaven National Laboratory, Upton, NY 11973, United States
* Corresponding authors

enhance its reducibility and improve the catalytic performance are quite desirable. The reduction temperature usually plays a significant role in the catalytic activity and stability of Co/TiO_2: large amounts of coke formed and led to significant deactivation as reduced below 1123 K, while higher reduction temperature would reduce coke deposition [8]. Ewbank et al. [9] reported that preparation methods for Co/γ-Al_2O_3 would also affect the particle size as well as dispersion and thus the activity and stability, due to the formation of two types of carbonaceous deposits, i.e., non-deactivating and deactivating coke. In addition, alloying cobalt with noble metals like Ru [10] and Pt [11] seems to also provide the improvement. This is because the formed Co-noble metals bimetallic interactions usually exhibit unique electronic properties compared to the corresponding parent metals, which in turn might enhance the catalytic performance [12].

In the present work, we adopted four different model surfaces, i.e., Pt-ter-PtCo(111), Pt(111), mixed-PtCo(111) and Co(001), to explore the synergistic effect of Pt-Co for the dry reforming of methane. To achieve this, first principle calculations were carried out to provide the *ab initio* insights in terms of molecular or atom. The results showed that the Pt-ter-PtCo(111) surface is more active than the monometallic as well as mixed surfaces.

2. Computational Method

Spin polarized density functional theory [13, 14] calculations were performed using the Vienna Ab-Initio Simulation Package (VASP) code [15, 16]. Projector augmented wave potentials were used to describe the core electrons with the generalized gradient approximation (GGA) [17, 18] using PW91 functionals [19]. The Kohn-Sham one-electron wave functions were expanded by using a plane wave basis set with a kinetic energy cutoff of 400 eV. The Brillouin zone was sampled using a $3 \times 3 \times 1$ k-point grid in the Monkhorst-Pack scheme [20]. Ionic positions were optimized until Hellman-Feynman force on each ion was smaller than 0.02 eV/Å.

The Pt(111) surface was modeled using a four layer 3×3 surface slab. The Pt(111) surface was modified by replacing subsurface (2nd layer) Pt atoms with Co atoms to model Pt-terminated-PtCo(111) surface (Pt-ter-PtCo(111) surface hereafter). The mixed-PtCo(111) surface was modeled using a four layer 4×4 surface slab. The Pt(111) surface was modified by replacing half of the Pt atoms in the top two layers with Co atoms to model mixed-PtCo(111) surface. The Co(001) surface was modeled using a four layer 3×3 surface slab. A 14 Å thick vacuum was added along the direction perpendicular to the surface in the initial slab model to avoid the artificial interactions between the slab and its periodic images. During geometry optimization, the atoms in the top two layers were allowed to relax while the atoms in the bottom two layers were fixed. The binding energy (BE) of an adsorbate, Gibbs free energy (G) of a species and change in free energy (ΔG) are calculated as follows:

$$BE(adsorbate) = E(slab + adsorbate) - E(slab) - E(adsorbate)\,, \qquad (1)$$

where *E(slab + adsorbate)*, *E(slab)* and *E(adsorbate)* are the total energies of the slab with adsorbate, clean slab and adsorbate species in the gas phase, respectively.

$$G = E + ZPE - TS\,. \tag{2}$$

Here, E is the total energy of a species obtained from DFT calculations, ZPE and S are the zero-point energy and entropy of a species respectively (T = 873 K). The ZPE and entropy of gas phase species were taken from NIST database [21].

$$\Delta G = \Delta E + \Delta ZPE - T\Delta S\,, \tag{3}$$

where ΔE is the binding energy of adsorbed species.

3. Results, Discussion and Conclusion

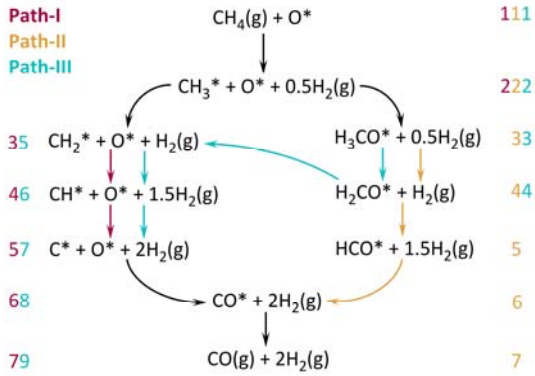

Scheme 1 Three possible pathways of methane reforming by O* to produce CO(g) and H_2(g). Note: the Arabic numerals in color refer to the steps along Path-I, Path-II, and Path-III, while the black lines represent the shared routes by different pathways.

Table 1. DFT calculated binding energies (in eV) of reaction intermediates on Pt, Co, and PtCo bimetallic surfaces.

Adsorbate	Pt(111)	Pt-ter-PtCo(111)	Mixed-PtCo(111)	Co(001)
O*	-4.11	-3.46	-5.25	-5.61
C*	-7.17	-6.39	-7.13	-7.07
CO*	-1.76	-1.10	-1.69	-1.70
HCO*	-2.46	-1.93	-2.62	-2.30
H_2CO*	-0.43	0.00	-0.96	-0.87
H_3CO*	-1.68	-1.49	-2.90	-2.99
CH*	-6.83	-5.77	-6.50	-6.47
CH_2*	-4.23	-3.46	-4.28	-4.14
CH_3*	-2.12	-1.68	-1.94	-2.07

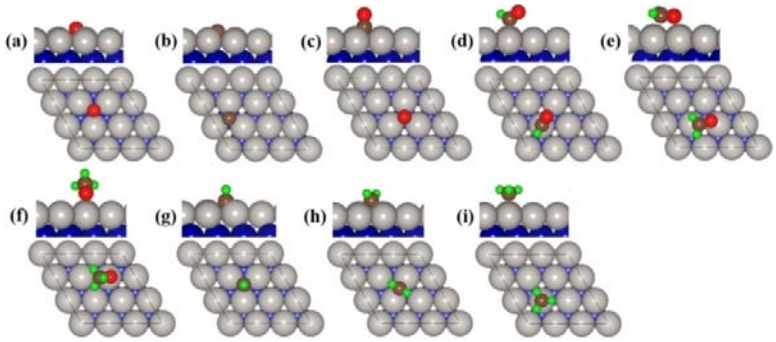

Fig. 1. Side and top views of DFT optimized geometries of O* (a), C* (b), CO* (c), HCO* (d), H_2CO* (e), H_3CO* (f), CH* (g), CH_2* (h), and CH_3* (i) on the Pt-ter-PtCo(111) surface. * = adsorbed species. Pt: grey, Co: blue, O: red, C: brown and H: green.

DFT calculations were performed to calculate the free energy diagrams for methane reforming by O* (assumed to be produced via CO_2* dissociation to CO* + O*) to produce CO(g) and H_2(g) at the temperature of 873 K along three possible reaction pathways shown in **Scheme 1**. To this end, the binding energies of reaction intermediates calculated on Pt(111), Pt-ter-PtCo(111), mixed-PtCo(111) and Co(001) surfaces (**Fig. 1** and **Table 1**) were used to calculate the free energy change along the reaction pathways in **Scheme 1**. Along the reaction Path-I, CH_4(g) undergoes consecutive C-H bond scission reactions to form C* which reacts with O* to form CO*. Along the reaction Path-II, CH_3* produced from the initial C-H bond scission of CH_4(g) reacts with O* to form H_3CO*. H_3CO* then undergoes consecutive C-H bond scission reactions to produce CO*. Along the reaction Path-III, H_2CO* formed through a similar route as in path-II undergoes C-O bond dissociation to form CH_2* and O*. CH_2* is then dehydrogenated to C* which reacts with O* to form CO*. Finally, CO* is desorbed as CO(g) and H_2(g) is formed due to the successive C-H bond scission of CH_x* of H_xCO* species in all reaction pathways shown in **Scheme 1**.

The DFT-calculated free energy diagrams in **Fig. 2** show that Path-I is the most energetically favorable reaction pathway for methane reforming on Pt(111), mixed-PtCo(111) and Co(001) surfaces while Path-II is the most energetically favorable reaction pathway for methane reforming on Pt-ter-PtCo(111). The most favorable reaction pathways (Path-I on Pt(111), mixed-PtCo(111) and Co(001) and Path-II on Pt-ter-PtCo(111) are plotted in **Fig. 3**. It shows that initial C-H bond scission of CH_4(g) (step 1→2 transition) is uphill in energy on all surfaces and likely is the rate-determining step (RDS). Furthermore, the ΔG values for step 1→2 transition on all the surfaces are very similar (**Fig. 3**). However, the Pt-ter-PtCo(111) surface lies much lower in energy compared to Pt(111), mixed-PtCo(111) and Co(001) surfaces for subsequent reaction steps 5, 6 and 7 (**Fig. 3**). Therefore, the bimetallic Pt-ter-PtCo(111) surface is predicted to demonstrate Pt-Co synergistic effect, and more active for methane reforming compared to the Pt(111), mixed-PtCo(111) and Co(001) surfaces.

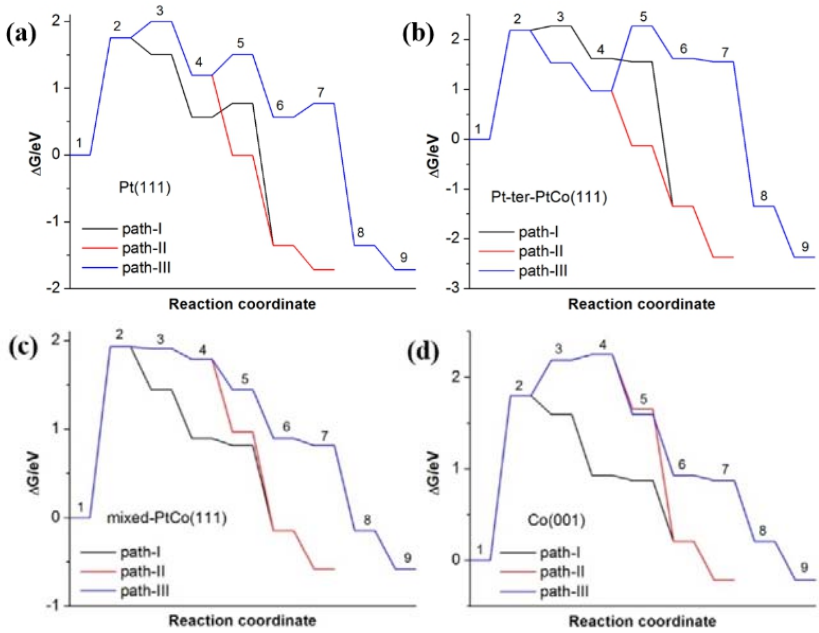

Fig. 2. DFT-calculated free energy diagrams for methane reforming by O* to produce CO(g) and H_2(g) (T = 873K) along three possible pathways shown in **Scheme 1**.

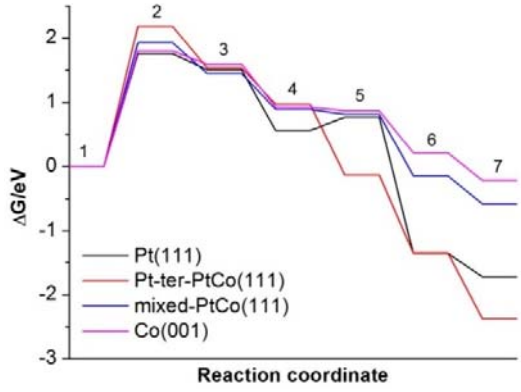

Fig. 3. DFT-calculated free energy diagrams for methane reforming by O* to produce CO(g) and H_2(g) (T = 873K) along the most favorable pathways.

Acknowledgement

This work was supported by the National Natural Science Foundation of China (Grant No. 51206200), and the Fundamental Research Funds for the Central Universities (Grant No. 106112016CDJZR145507). The DFT calculations were performed using computational resources at the Center for Functional Nanomaterials, a user

facility at Brookhaven National Laboratory.

References

[1] L. Shi, G. Yang, K. Tao, Y. Yoneyama, Y. Tan, N. Tsubaki: *An Introduction of CO_2 Conversion by Dry Reforming with Methane and New Route of Low-Temperature Methanol Synthesis.* Accounts of Chemical Research. *46*, (2013) 1838–47.

[2] J. K. Dahl, A. W. Weimer, A. Lewandowski, C. Bingham, F. Bruetsch, A. Steinfeld: *Dry Reforming of Methane Using a Solar-Thermal Aerosol Flow Reactor.* Industrial & Engineering Chemistry Research. (2004), 5489–95.

[3] D. Pakhare, J. Spivey.: *A review of dry (CO_2) reforming of methane over noble metal catalysts.* Chemical Society reviews. *43* (2014), 7813–37.

[4] J. Gao, Z. Hou, H. Lou, X. Zheng: *Dry (CO_2) Reforming.* Fuel Cell (2011), 191–221.

[5] A. W. Budiman, S. H. Song, T. S. Chang, C. H. Shin, M. J. Choi: *Dry Reforming of Methane Over Cobalt Catalysts: A Literature Review of Catalyst Development.* Catalysis Surveys from Asia. *16* (2012), 183-=97.

[6] G. Jones, J. G. Jakobsen, S. S. Shim, J. Kleis, M. P. Andersson, J. Rossmeisl, et al.: *First principles calculations and experimental insight into methane steam reforming over transition metal catalysts.* Journal of Catalysis. *259* (2008). 147–60.

[7] E. Ruckenstein, H. Y. Wang: *Carbon Deposition and Catalytic Deactivation during CO_2 Reforming of CH_4 over Co/γ-Al_2O_3 Catalysts.* Journal of Catalysis. *205* (2002), 289-93.

[8] K. Nagaoka: *Influence of the reduction temperature on catalytic activity of Co/TiO_2 (anatase-type) for high pressure dry reforming of methane.* Applied Catalysis A: General. *255* (2003), 13–21.

[9] J. L. Ewbank, L. Kovarik, C. C. Kenvin, C. Sievers: *Effect of preparation methods on the performance of Co/Al_2O_3 catalysts for dry reforming of methane.* Green Chem. *16* (2014), 885–96.

[10] K. Nagaoka: *Modification of Co/TiO_2 for dry reforming of methane at 2MPa by Pt, Ru or Ni.* Applied Catalysis A: General. *268* (2004), 151–8.

[11] M. Myint, B. Yan, J. Wan, S. Zhao, J. G. Chen: *Reforming and oxidative dehydrogenation of ethane with CO_2 as a soft oxidant over bimetallic catalysts.* Journal of Catalysis. *343* (2016), 168–77.

[12] W. Yu, M. D. Porosoff, J. G. Chen: *Review of Pt-based bimetallic catalysis: from model surfaces to supported catalysts.* Chemical reviews. *112* (2012), 5780–817.

[13] P. Hohenberg, W. Kohn: (1964) *Inhomogeneous Electron Gas.* Physical Review. 136 (1964), B864.

[14] W. Kohn, L. J. Sham: *Self-Consistent Equations Including Exchange and Correlation Effects.* Physical Review. *140* (1965), A1133–A8.

[15] G. Kresse, J. Furthmüller: *Efficiency of ab-initio total energy calculations for metals and semiconductors using a plane-wave basis set.* Computational Materials Science. *6* (1996), 15-50.

[16] G. Kresse, J. Hafner. A. B. initio: Physical Review B. *48* (1993), 13115-,8.

[17] G. Kresse, D. Joubert: *From ultrasoft pseudopotentials to the projector augmented-wave method.* Physical Review B. *59* (1999), 1758-75.

[18] P. E. Blöchl.: *Projector augmented-wave method.* Physical Review B. *50* (1994), 17953,-79.

[19] J. P. Perdew, Y. Wang: *Pair-distribution function and its coupling-constant average for the spin-polarized electron gas.* Physical Review B. *46* (1992), 12947-,54.

[20] H. J. Monkhorst, J. D. Pack: *Special points for Brillouin-zone integrations.* Physical Review B. *13* (1976) 5188–92.

[21] *Computational Chemistry Comparison and Benchmark DataBase; http://cccbdbnistgov.*

Received May 7, 2017